Available online at www.sciencedirect.com
ScienceDirect
Journal of Molecular Structure 886 (2008) 148–157
Journal of MOLECULAR STRUCTURE
www.elsevier.com/locate/molstruc

X-ray, FT-Raman, FT-IR spectra and ab initio HF, DFT calculations of 2-[(5-methylisoxazol-3-yl)amino]-2-oxo-ethyl methacrylate

Mehmet Karabacak [a,*], Ertan Şahin [b], Mehmet Çınar [a], İbrahim Erol [c], Mustafa Kurt [d]

[a] Department of Physics, Afyonkarahisar Kocatepe University, 03040 Afyonkarahisar, Turkey
[b] Department of Chemistry, Atatürk University, 25240 Erzurum, Turkey
[c] Department of Chemistry, Afyonkarahisar Kocatepe University, 03040 Afyonkarahisar, Turkey
[d] Department of Physics, Ahi Evran University, 40100 Kırşehir, Turkey

Received 1 August 2007; received in revised form 1 November 2007; accepted 8 November 2007
Available online 21 November 2007

Abstract

Molecular structure of methacrylate monomer, 2-[(5-methylisoxazol-3-yl)amino]-2-oxo-ethyl methacrylate (IAOEMA) was determined by X-ray diffraction analysis. The molecule (IAOEMA) crystallizes in monoclinic, space group $P2_1/c$ (no: 14) with $a = 11.927(5)$, $b = 5.312(2)$, $c = 17.278(6)$ Å, $V = 1092.4(1)$ Å^3 and four molecules in the unit cell. In the structure, five-membered isoxazole ring is a planer; acetamide and acetate carbonyl bond lengths are 1.213(2) and 1.208(2) Å. Furthermore, FT-IR and FT-Raman spectra of the molecule were measured. The molecular geometry, vibrational frequencies, infrared intensities and Raman scattering activities of IAOEMA in the ground state have been calculated by using ab initio Hartree-Fock (HF) and density functional (B3LYP and B3PW91) methods with the 6-31G(d,p) and 6-311G(d,p) basis sets. The vibrational frequencies were calculated and scaled values have been compared with experimental FT-IR and FT-Raman spectra. The observed and calculated frequencies are found to be in good agreement. The optimized bond lengths and bond angles show the best agreement with the experimental results.

Keywords: Ab initio and DFT; 2-[(5-Methylisoxazol-3-yl)amino]-2-oxo-ethyl methacrylate; Crystal structure; FT-IR and FT-Raman spectrum; Vibrational frequencies

1. Introduction

Acrylate and methacrylate have figured prominently in the development of soft-tissue-compatible materials and orthopedic and dental cements. Acrylate and methacrylate vinyl esters are readily polymerized by free radical polymerization (FRP) to form linear, branched, or network polymers [1].

Nowadays, synthesis of functional monomers and their polymers and use in synthesis of new functional polymers have attracted considerable interest. Methacrylic polymers find extensive applications in fiber optics, metal complexes, polymeric reagents, and polymeric supports [2,3].

IAOEMA is a new methacrylate monomer having pendant isoxazole group. In previous [4,5] studies, the synthesis, characterization, copolymerizations behavior and biological activity of IAOEMA were described. In the present work, we have determined the crystal structure of IAOEMA by single crystal X-ray diffraction. FT-IR and FT-Raman spectra of compound were recorded. We have calculated the theoretical vibrational frequencies of IAOEMA in the ground state to distinguish fundamentals from experimental vibrational frequencies and geometric parameters using Hartree-Fock (HF) and Density Functional Theory (DFT) methods using B3LYP (Becke 3-Lee-Yang-Parr) and B3PW91 (Becke 3-Perdew-Wang 91) functional [6] with the 6-31G(d,p), 6-31+G(d,p), 6-31++G(d,p), 6-311G(d,p), 6-311+G(d,p), and 6-311++G(d,p) basis sets. These experimental and calculated values are

* Corresponding author. Tel.: +90 272 2281311; fax: +90 272 2281235.
E-mail address: karabacak@aku.edu.tr (M. Karabacak).

0022-2860/$ - see front matter © 2007 Elsevier B.V. All rights reserved.
doi:10.1016/j.molstruc.2007.11.014

valuable for providing insight into the vibrational spectrum and molecular parameters. The purpose of the present study is to show the results of X-ray diffraction, FT-IR and FT-Raman spectra and to calculate optimal molecular geometry, vibrational frequencies and normal modes associated of IAOEMA and to find effective methods that would offer a higher certainty of finding vibrational wavenumbers and molecular parameters.

Ab initio HF and DFT has become a powerful tool in the investigation of vibrational spectra and molecular structure (bond lengths and bond angles) [6–9]. Based on experimental data of 20 small organic molecules, Rauhut and Pulay have indicated that B3LYP method leads to geometry parameters near to experimental data [9]. Therefore, we expect that B3LYP calculated geometry of studied molecule is in good agreement with their experimental geometric parameters.

In the present study, experimental geometric parameters with X-ray diffraction, FT-IR and FT-Raman spectra of IAOEMA were examined and in the ground state theoretical geometric parameters, IR and Raman spectra of IAOEMA were calculated by using Gaussian 03 suite of quantum chemical codes [10], for the first time. A detailed quantum chemical study will aid in making definite assignments to fundamental normal modes of IAOEMA and in clarifying the experimental data for this important molecule. Ab initio HF and DFT calculations have been performed to support our vibrational assignments.

2. Experimental

The preparation technique of IAOEMA is explained in previous study [4]. In this study we have determined crystal structure and vibrational frequencies of this compound using X-ray, FT-Raman and FT-Infrared spectroscopy.

2.1. X-ray structure determination

For crystal structure determination, the single-crystal of the compound IAOEMA was used for data collection on a four-circle Rigaku R-AXIS RAPID-S diffractometer equipped with a two-dimensional area IP detector. The graphite-monochromatized Mo Kα radiation ($\lambda = 0.71073$ Å) and oscillation scans technique with $\Delta\omega = 5°$ for one image were used for data collection. The lattice parameters were determined by the least-squares methods on the basis of all reflections with $F^2 > 2\sigma(F^2)$. Integration of the intensities, correction for Lorentz and polarization effects and cell refinement was performed using CrystalClear (Rigaku/MSC Inc., 2005) software [11]. The structure was solved by the direct method using SHELXS [12]. The positional and atomic displacement parameters (ADPs) were refined by the full-matrix least-squares method using SHELXL [12]. The H atoms were positioned geometrically and constrained to ride on their parent atom except the N5–H hydrogen atom that was located in difference map. The final difference Fourier maps showed no peaks of chemical significance. The details of the data collection and final refinement parameters are listed in Table 1.

2.2. FT-IR and FT-Raman spectra

Infrared spectrum of compound was recorded between 4000 and 400 cm^{-1} on a Perkin-Elmer FT-IR System Spectrum BX spectrometer which was calibrated using polystyrene bands and fewer than 400 cm^{-1} on Bruker IFS 66/S spectrometer. The sample was finely ground and mixed with KBr. This mixture was then pressed under vacuum at high pressure to obtain a transparent disc, which was then placed in the sample compartment. The spectrum was recorded at room temperature, with a scanning speed of 10 cm^{-1} min^{-1} and the spectral resolution of 4.0 cm^{-1}. FT-Raman spectra of the samples were recorded using 1064 nm line of Nd:YAG laser as excitation wave length in the region 3500–50 cm^{-1} on a Bruker FRA 106/S FT-Raman. The detector is a liquid nitrogen cooled Ge detector.

3. Quantum chemical calculations

In recent years, ab initio HF and DFT have become a powerful tool in the investigation of molecular structure and vibrational spectra [13]. The molecular structure of

Table 1
Crystal data and structure refinement for IAOEMA

Chemical formula	$C_{10}H_{12}N_2O_4$
Formula weight	224.2
Temperature (K)	293(2)
Wavelength (Å)	0.71073
Crystal system, space group	Monoclinic, $P2_1/c$
Unit cell dimensions (Å,°)	
a	11.927(5)
b	5.312(2)
c	17.278(6)
β	95.05(2)
Volume (Å^3)	1092.4(1)
Z	4
Density (calculated)	1.37 Mg/m^3
bsorption coefficient (mm^{-1})	0.107
$F(000)$	472
Crystal size (mm^3)	0.20, 0.17, 0.15
θ Range for collection (°)	2.4–30.6
Index ranges	$-16 \leqslant h \leqslant 17$, $-7 \leqslant k \leqslant 6$, $-24 \leqslant l \leqslant 24$
Refl. Collected	29708
Independent reflections	3343 ($R_{int} = 0.068$)
Observed reflections	1799($I > 2\sigma$ I)
Parameters	151
Goodness-of-fit on F^2	1.027
Final R indices [$I > 2\sigma(I)$]	
R_1	0.062
wR_2	0.157
Largest diff. peak and hole (Å^{-3})	0.130 and 0.216

$R_1 = \sum \| |F_0| - |F_c| \| / \sum |F_0|, wR_2 = \left\{ \sum \left[w(F_0^2 - F_c^2)^2 \right] / \sum \left[w(F_0^2)^2 \right] \right\}^{1/2}$.

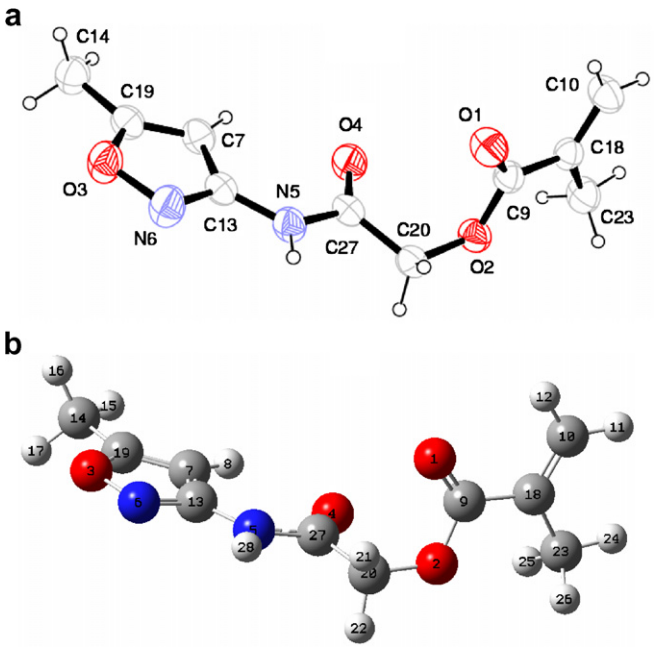

Fig. 1. (a) The molecular structure of IAOEMA, showing the atom–labelling scheme. Displacement ellipsoids are drawn at the 50% probability level. (b) Optimized geometry of IAOEMA structure and atoms numbering.

IAOEMA in the ground state (*in vacuo*) is determined HF, B3LYP and B3PW91 employing the 6-31G(d,p), 6-31+G(d,p), 6-31++G(d,p), 6-311G(d,p), 6-311+G(d,p), and 6-311++G(d,p) basis sets. There are no significant difference geometric parameters and vibrational frequencies by the selection of the different basis sets. The optimized structural parameters were used in the vibrational frequency calculations at HF and DFT levels. The calculated vibrational frequencies are scaled by 0.9026, 0.9085 for HF, 0.9608, 0.9668 for B3LYP and 0.9584, 0.9631 for B3PW91 for 6-31G(d,p) and 6-311G(d,p) basis sets, respectively [14]. The theoretical results have enabled us to make the detailed assignments of the experimental IR and Raman spectra of IAOEMA. Molecular geometry is not restricted and all the calculations are performed by using GaussView molecular visualisation program [15] and *GAUSSSIAN 03* program package on the personal computer [10].

4. Results and discussion

4.1. Crystal structure

The molecular structure of IAOEMA with the atom labeling is shown in Fig. 1, and the bond lengths and bond angles are listed in Tables 2 and 3, respectively. In the

Table 2
Bond lengths (Å) experimental and optimized for IAOEMA

Parameters	X-ray	6-31G(d,p)			6-311G(d,p)		
		HF	B3LYP	B3PW91	HF	B3LYP	B3PW91
Bond lengths							
O(1)–C(9)	1.208(2)	1.189	1.213	1.212	1.183	1.206	1.205
O(2)–C(9)	1.347(2)	1.335	1.365	1.360	1.333	1.364	1.358
O(2)–C(20)	1.432(2)	1.397	1.418	1.412	1.395	1.418	1.411
O(3)–N(6)	1.412(2)	1.369	1.400	1.386	1.363	1.396	1.383
O(3)–C(19)	1.337(2)	1.323	1.352	1.347	1.320	1.349	1.344
O(4)–C(27)	1.213(2)	1.191	1.216	1.215	1.186	1.209	1.208
N(5)–C(13)	1.392(2)	1.385	1.393	1.388	1.386	1.392	1.387
N(5)–C(27)	1.358(2)	1.364	1.376	1.372	1.364	1.376	1.372
N(5)–H(28)	0.83(2)	0.996	1.012	1.011	0.995	1.011	1.010
N(6)–C(13)	1.306(2)	1.285	1.318	1.317	1.282	1.313	1.312
C(7)–H(8)	0.930	1.065	1.076	1.076	1.065	1.074	1.075
C(7)–C(13)	1.404(3)	1.427	1.425	1.421	1.428	1.424	1.420
C(7)–C(19)	1.348(3)	1.344	1.363	1.362	1.343	1.360	1.360
C(9)–C(18)	1.473(3)	1.494	1.494	1.491	1.495	1.495	1.491
C(10)–H(11)	0.930	1.075	1.085	1.086	1.076	1.084	1.085
C(10)–H(12)	0.930	1.074	1.084	1.085	1.074	1.083	1.084
C(10)–C(18)	1.341(3)	1.322	1.339	1.338	1.320	1.335	1.334
C(14)–H(15)	0.960	1.082	1.091	1.091	1.082	1.090	1.090
C(14)–H(16)	0.960	1.084	1.095	1.095	1.085	1.093	1.094
C(14)–H(17)	0.960	1.084	1.095	1.095	1.085	1.093	1.094
C(14)–C(19)	1.477(3)	1.489	1.489	1.485	1.488	1.487	1.482
C(18)–C(23)	1.466(3)	1.507	1.506	1.501	1.506	1.505	1.499
C(20)–H(21)	0.970	1.082	1.095	1.095	1.082	1.093	1.094
C(20)–H(22)	0.970	1.083	1.094	1.094	1.082	1.092	1.093
C(20)–C(27)	1.514(3)	1.523	1.537	1.532	1.523	1.536	1.531
C(23)–H(24)	0.960	1.083	1.093	1.093	1.083	1.091	1.092
C(23)–H(25)	0.960	1.084	1.095	1.095	1.085	1.093	1.094
C(23)–H(26)	0.960	1.085	1.095	1.095	1.085	1.093	1.094
σ (RMS)		0.087	0.094	0.094	0.087	0.093	0.093

Table 3
Bond angles (°) experimental and optimized for IAOEMA

Parameters	X-ray	6-31G(d,p)			6-311G(d,p)		
		HF	B3LYP	B3PW91	HF	B3LYP	B3PW91
Bond angles							
C(9)–O(2)–C(20)	115.6(2)	116.6	114.9	114.6	117.1	115.5	115.2
N(6)–O(3)–C(19)	109.2(2)	109.7	109.5	109.7	109.8	109.4	109.7
C(13)–N(5)–C(27)	125.1(2)	126.0	125.9	125.8	126.0	126.0	125.9
C(13)–N(5)–H(28)	118.9(2)	114.6	114.7	114.7	114.6	114.6	114.6
C(27)–N(5)–H(28)	116.0(2)	119.4	119.4	119.5	119.3	119.3	119.4
O(3)–N(6)–C(13)	104.6(2)	105.5	104.6	104.8	105.7	104.8	105.0
H(8)–C(7)–C(13)	127.7	128.1	127.3	127.5	128.2	127.4	127.5
H(8)–C(7)–C(19)	127.7	129.7	129.6	129.7	129.7	129.5	129.6
C(13)–C(7)–C(19)	104.7(2)	102.2	103.1	102.9	102.1	103.1	102.9
O(1)–C(9)–O(2)	121.5(2)	122.2	122.4	122.5	122.4	122.5	122.6
O(1)–C(9)–C(18)	126.4(2)	125.7	126.3	126.2	125.8	126.3	126.3
O(2)–C(9)–C(18)	112.1(2)	112.0	111.3	111.3	111.8	111.1	111.1
H(11)–C(10)–H(12)	120.0	117.8	118.1	118.3	117.8	118.2	118.3
H(11)–C(10)–C(18)	120.0	121.3	121.4	121.4	121.3	121.4	121.3
H(12)–C(10)–C(18)	120.0	120.9	120.5	120.4	120.9	120.5	120.3
N(5)–C(13)–N(6)	117.4(2)	118.2	117.8	117.8	118.3	117.9	117.9
N(5)–C(13)–C(7)	130.5(2)	129.6	129.4	129.5	129.6	129.4	129.6
N(6)–C(13)–C(7)	112.2(2)	112.2	112.8	112.7	112.1	112.6	112.5
H(15)–C(14)–H(16)	109.5	109.0	108.7	108.6	109.1	108.7	108.7
H(15)–C(14)–H(17)	109.5	109.1	108.7	108.7	109.2	108.7	108.7
H(15)–C(14)–C(19)	109.5	110.3	110.1	110.1	110.2	110.1	110.1
H(16)–C(14)–H(17)	109.5	108.0	107.6	107.7	108.1	107.7	107.7
H(16)–C(14)–C(19)	109.5	110.2	110.9	110.9	110.1	110.7	110.7
H(17)–C(14)–C(19)	109.5	110.2	110.9	110.9	110.1	110.7	110.7
C(9)–C(18)–C(10)	117.4(2)	116.8	116.8	116.6	116.9	116.9	116.7
C(9)–C(18)–C(23)	119.7(2)	118.8	119.0	119.0	118.8	118.9	119.0
C(10)–C(18)–C(23)	122.9(2)	124.4	124.2	124.3	124.3	124.2	124.3
O(3)–C(19)–C(7)	109.4(2)	110.4	110.0	109.9	110.4	110.0	109.9
O(3)–C(19)–C(14)	116.6(2)	116.9	116.7	116.7	117.0	116.8	116.9
C(7)–C(19)–C(14)	134.0(2)	132.8	133.3	133.3	132.6	133.2	133.2
O(2)–C(20)–H(21)	109.4	111.0	110.7	110.7	111.1	110.6	110.7
O(2)–C(20)–H(22)	109.4	106.3	105.8	106.0	106.3	105.9	106.0
O(2)–C(20)–C(27)	111.2(2)	111.0	110.8	110.7	111.1	110.8	110.8
H(21)–C(20)–H(22)	108.0	109.4	109.7	109.6	109.5	109.8	109.8
H(21)–C(20)–C(27)	109.4	110.4	110.3	110.3	110.2	110.1	110.1
H(22)–C(20)–C(27)	109.4	108.6	109.4	109.4	108.5	109.5	109.4
C(18)–C(23)–H(24)	109.5	110.2	110.6	110.6	110.1	110.6	110.6
C(18)–C(23)–H(25)	109.5	110.9	110.9	110.9	110.8	110.7	110.7
C(18)–C(23)–H(26)	109.5	111.3	111.3	111.3	111.2	111.2	111.2
H(24)–C(23)–H(25)	109.5	108.6	108.7	108.7	108.7	108.8	108.8
H(24)–C(23)–H(26)	109.5	108.5	108.6	108.6	108.6	108.7	108.7
H(25)–C(23)–H(26)	109.5	107.3	106.7	106.7	107.3	106.7	106.7
O(4)–C(27)–N(5)	123.9(2)	124.4	124.4	124.4	124.5	124.5	124.5
O(4)–C(27)–C(20)	123.3(2)	122.7	122.8	122.8	122.8	122.9	122.9
N(5)–C(27)–C(20)	112.8(2)	112.9	112.8	112.8	112.7	112.6	112.5
σ (RMS)		1.428	1.440	1.437	1.426	1.413	1.409

structure, five-membered isoxazole ring is a planer, acetamide and acetate carbonyl bond lengths are 1.213(2) and 1.208(2) Å, respectively. The C–C distances are in the range 1.404(2)–1.514(2) Å, this large display indicating a partial loss of π-delocalisation. Terminal moieties are considerably twisted along the O2–C20–C27 atomic axis. This is attributed to the short intermolecular N–H···O contact [N5–H···O1 = 2.907(4) Å, <N5–H···O1 = 168°] present in the molecule. Atom N5 of the amide group in the molecule at (x, y, z) acts as a hydrogen bond donor to carbonyl atom O1 in the molecule at $(-x, 1/2 + y, 1/2 - z)$, producing a chain. Molecules within the chains are arranged in an antiparallel manner and are stabilized by the second hydrogen bond [C10–H···N6 $(-x, -1/2 + y, 1/2 - z) = 3.518(4)$ Å, <N5–H···O1 = 164°].

4.2. Optimized structure

The first task for a computational work was to determine the optimized geometry of IAOEMA. The optimized structure parameters calculated ab initio HF and DFT (B3LYP and B3PW91) with the 6-31G(d,p) and

6-311G(d,p) basis sets listed in Tables 2 and 3 in accordance with the atom numbering scheme given in Fig. 1(b).

The optimized parameters obtained by HF, B3LYP and B3PW91 methods are approximately similar. It is well known that HF method under estimate some bond lengths [16]. As seen from Table 2, the C–O, N–O and C–N distances (except for C27–N5) are calculated at HF level of theory with a value smaller than the experimental value, comparing with B3LYP and B3PW91 level of theory. Using these methods similar calculations were found for ethylene methacrylate [17] and 1-amino-5-benzoyl-4-phenylpyrimidin-2(1H) [18].

Taking into account that the molecular geometry in the vapour phase may be different from in the solid phase, owing to extended hydrogen bonding and stacking interactions there is reasonable agreement between the calculated and experimental geometric parameters. As discussed by Johnson et al. [19], DFT method predicts bond lengths which are systematically too long, particularly the C–H bond lengths. This theoretical pattern also found for IAOEMA. Since the large deviation from experimental C–H bond lengths may arise from the low scattering of hydrogen atoms in X-ray diffraction experiment. For example, C–H bond lengths values in the experiment are 0.93, 0.96 and 0.97 Å but the values in the theoretical results are bigger than 1 Å. Using these methods similar calculations were found for 2,20-biquinoline [20] and 2,4-dinitrophenylhydrazine [21].

The optimized N–H bond length by HF and DFT with 6-31G(d,p) and 6-311G(d,p) methods is from 0.995 to 1.012 Å. By comparing these values with experimental value of 0.83(2) Å, it is observed that HF method estimate the N–H bond length better than other methods.

Experimental values of C–O bond length compare with the optimized bond length of C–O by HF and DFT methods, HF method underestimate C–O bond length where as DFT methods overestimate the same.

The optimized bond lengths of C–C in ring in the range from 1.343 to 1.428 Å for HF, 1.360 to 1.425 Å for B3LYP and 1.359 to 1.421 Å for B3PW91 with 6-31G(d,p) and 6-311G(d,p) methods which are in good agreement with those in crystal structure (1.348–1.404 Å). The C–CH_3 bond length is slightly overestimated whereas the C–CH_2 bond length is underestimated all the levels.

The N–C–C angle is larger than other angles in the ring. The optimized bond angles of the ring fall in the range from 104° to 112°. These angles are comparing with experimental values which are approximately the same.

To make comparison with experimental data, we present RMS (σ) values based on the calculations bottom of Tables 2 and 3. As seen in Tables 2 and 3, the bond lengths values calculated by means of HF method are the closest to experimental data and HF method correlates well for bond lengths. Bond angles values calculated by means of B3PW91 method are the closest to experimental data and B3PW91 method correlates well for bond angles compared with other methods. The best RMS bond length vaslue is about 0.087 for HF/6-31G(d,p) and 6-311G(d,p) level of theory for IAOEMA, and bond angle value is also about 1.409 for B3PW91 method with 6-311G(d,p) for IAOEMA.

4.3. Vibrational spectra

The present molecule IAOEMA has C_1 point group symmetry. The molecule has 28 atoms and 78 normal modes of vibrations. The modes have been assigned according to the detailed motion of the individual atoms. Optimized ground-state vibrational modes for studied molecular structure were obtained by ab initio HF and DFT (B3LYP and B3PW91) with the 6-31G(d,p) and 6-311G(d,p) basis sets and compared with the experimental frequencies.

FT-IR and FT-Raman spectra are shown in Fig. 2. The simulated infrared and Raman spectra are shown in Fig. 3, where the calculated intensities (IR) and scattering Raman activities are plotted against the vibrational frequencies. Theoretical infrared spectra have revealed more pronounced differences with the experimental FT-IR spectrum, as shown in Figs. 2 and 3. It must be due to the fact that hydrogen bond vibrations present in crystal lead to strong perturbation of infrared intensities (and frequencies) of many other modes. In FT-IR spectrum (in the region of 1800–3400 cm^{-1}) the complicated pattern of absorption originates from the N–H stretching mode. Furthermore, a number of combinations are observed in this region of the spectrum. The resulting vibrational frequencies for the optimized geometries and the proposed

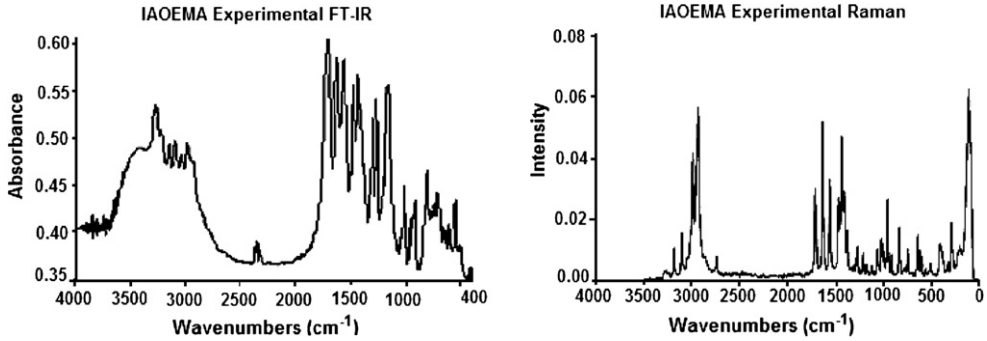

Fig. 2. Experimental FT-IR and FT-Raman spectra of IAOEMA.

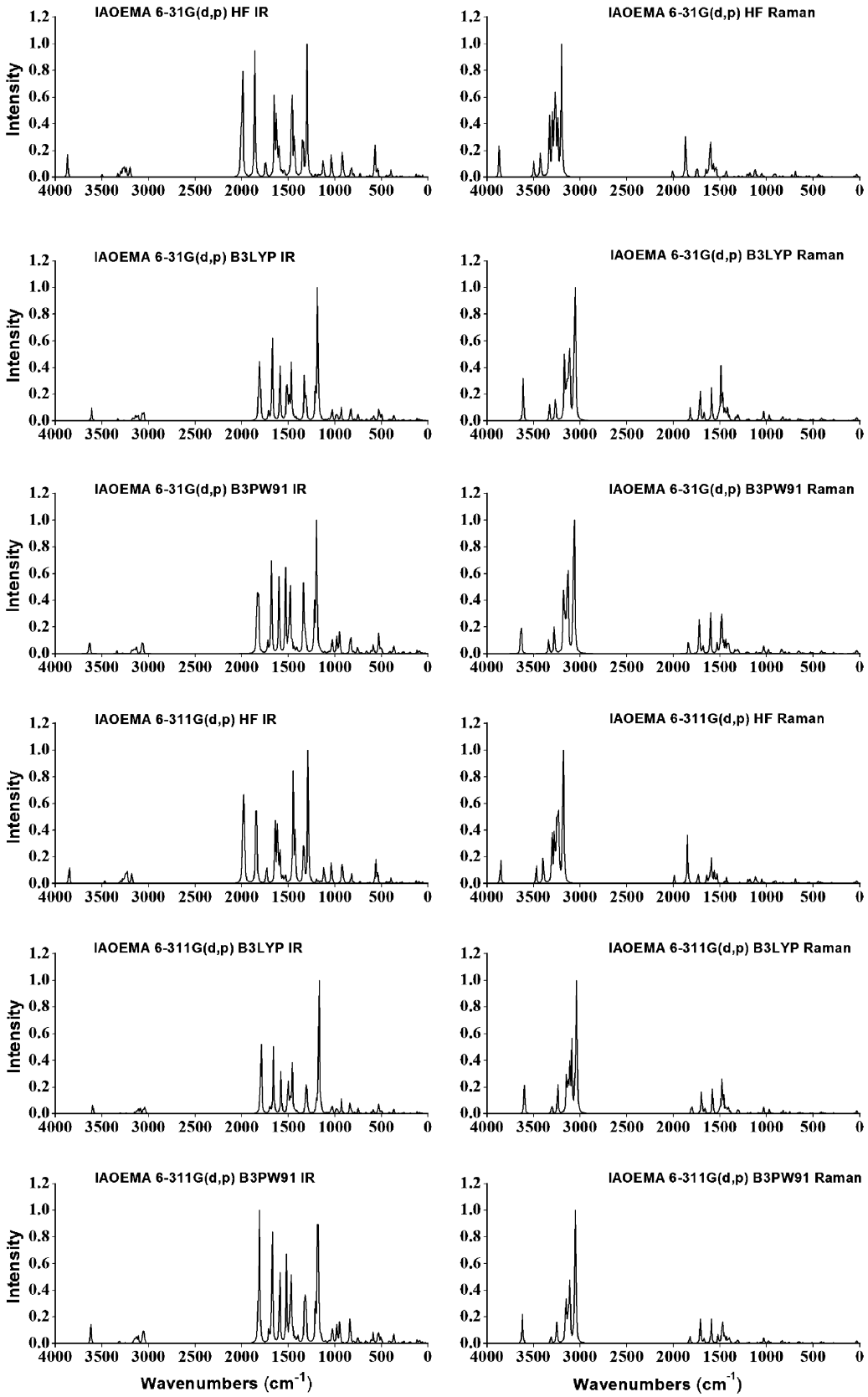

Fig. 3. Comparison of calculated frequencies in cm^{-1} normalized IR intensities and Raman activities at each level of theory considered for IAOEMA. These theoretical spectrum were obtained by using HF and DFT (B3LYP and B3PW91) methods with two basis sets (6-31G(d,p) and 6-311G(d,p)).

Table 4
Comparison of the calculated and experimental (FT-IR and FT-Raman) vibrational spectra of free IAOEMA

	6-31G(d,p)									6-311G(d,p)									Experimental In this study	Approximate assignments
	HF			B3LYP			B3PW91			HF			B3LYP			B3PW91				
	Freq[a]	I(IR)	I(Ra)	Freq[b]	I(IR)	I(Ra)	Freq[c]	I(IR)	I(Ra)	Freq[d]	I(IR)	I(Ra)	Freq[e]	I(IR)	I(Ra)	Freq[f]	I(IR)	I(Ra)	IR(Raman)	
1	19	0.4	1.9	16	0.3	2.1	16	0.3	2.1	20	0.4	1.7	17	0.3	1.9	17	0.3	1.8		$\rho CH_3+\rho CH_2$
2	30	2.0	6.2	32	1.0	6.5	31	1.1	6.8	31	1.9	5.7	30	1.2	7.1	30	1.1	6.9		$\rho CH_3+\rho CH_2$
3	34	0.4	0.9	35	1.0	2.6	36	0.9	2.2	34	0.4	0.8	35	0.6	1.6	36	0.7	1.7		ρCH_3
4	55	6.3	1.7	62	3.3	1.4	61	3.4	1.3	56	5.5	1.5	60	3.1	1.2	60	3.3	1.1		ρCH_2
5	71	2.3	0.9	72	2.1	1.3	72	1.8	1.4	69	2.3	0.8	72	2.1	1.2	72	2.0	1.2		τCH_3+ing wagging
6	94	7.0	0.4	89	4.7	0.4	87	4.5	0.4	92	7.0	0.3	87	6.0	0.3	87	5.8	0.3		$\tau CH_3+\rho$OC out of plane
7	113	1.4	0.1	96	3.0	0.2	94	3.4	0.2	116	1.2	0.1	100	2.0	0.2	97	2.4	0.2		τCH_3
8	119	8.4	0.5	116	7.9	0.7	115	8.3	0.7	118	8.8	0.5	115	8.5	0.8	115	8.8	0.8	(111)	ωCH_3
9	183	2.9	0.3	182	2.3	0.2	181	2.3	0.2	185	2.9	0.3	184	2.3	0.2	182	1.9	0.1		τCH_3
10	194	0.5	0.1	188	0.7	0.1	184	0.7	0.1	197	0.4	0.1	186	0.6	0.2	183	1.1	0.3		τCH_3
11	202	1.6	0.9	198	1.5	1.0	198	1.7	1.0	203	1.9	0.7	197	1.8	0.9	198	2.1	0.9		βC-CH_3
12	254	5.0	0.8	253	4.5	0.5	251	4.6	0.6	254	5.4	0.9	252	5.2	0.7	251	5.1	0.7		βC-CH_3
13	274	3.8	2.2	270	2.7	3.1	270	2.7	2.9	274	3.6	2.1	269	2.5	3.0	269	2.6	2.8		ρCH_2
14	310	4.0	1.2	304	2.9	1.5	302	2.9	1.4	311	3.7	1.0	306	2.7	1.2	304	2.6	1.2	(290)	βC-$CH_3+\beta$CO
15	359	25.7	1.9	352	21.7	1.3	352	23.3	1.4	361	23.0	1.7	355	19.6	1.3	355	21.5	1.4		$\omega CH_3+\rho\ CH_2$
16	373	0.9	0.6	361	2.6	0.8	362	1.0	0.7	376	1.1	0.4	361	2.3	0.7	363	0.6	0.5		$\rho CH_2+\beta$NH
17	378	3.8	2.3	373	2.0	2.2	370	1.7	2.2	379	3.5	2.4	376	2.1	2.4	372	1.9	2.4	374	βCCC
18	400	4.5	5.4	394	1.3	3.4	393	1.3	3.3	403	5.6	5.0	398	2.4	3.4	397	1.7	3.0		γCCC
19	407	3.2	1.9	399	5.6	4.2	398	5.9	4.3	410	3.8	1.9	403	6.1	3.8	401	7.0	4.1	417	βC-$CH_3+\beta$NH
20	490	29.4	3.3	483	20.5	3.1	484	20.4	3.0	492	30.5	3.0	488	17.6	3.1	488	18.4	3.0		βCCC+γNH
21	515	93.6	2.6	506	47.5	3.7	508	46.4	3.4	510	79.9	2.0	515	42.5	2.6	515	40.5	2.5	512	γNH+ρCH_2
22	565	7.9	1.6	561	23.5	1.5	562	27.4	1.4	569	5.9	1.6	567	23.4	1.4	567	25.9	1.3	556	γNH+ρCH_2
23	592	3.7	2.4	584	6.1	1.6	586	6.6	1.7	595	3.2	2.5	588	7.0	1.7	589	7.1	1.7	598	γNH+$\rho CH_2+\beta$CCC
24	623	1.0	5.3	604	0.3	2.8	607	0.2	2.7	625	0.8	5.5	609	0.1	2.4	611	0.0	2.3	617	γCCC+ρCH_2 of CH_3
25	624	0.1	4.2	621	0.8	4.3	623	1.0	4.3	629	0.2	3.6	623	0.5	4.4	626	0.6	4.3		νC-CH_3
26	660	11.0	3.8	637	7.4	4.7	636	7.4	4.6	666	9.6	1.8	645	7.0	2.7	642	7.3	2.6	(643)	tCH_2
27	721	9.0	0.3	684	4.0	0.3	684	3.6	0.3	725	5.0	0.3	692	2.6	0.3	691	2.3	0.3		γCH+γCCN
28	744	49.2	3.6	724	25.3	5.4	724	23.8	4.8	748	44.6	3.7	725	22.2	5.3	727	21.4	4.7	713	$tCH_2+\beta$CCO
29	774	3.9	3.1	760	5.2	3.9	764	4.7	3.8	777	4.3	2.6	764	6.1	3.6	767	5.2	3.4		βC-H+βCNO+βCNC
30	817	8.9	8.6	789	10.6	6.6	792	13.0	4.7	822	8.5	8.8	794	11.2	8.5	798	10.9	6.7		$tCH_2+\beta$OCO
31	829	52.8	1.3	800	14.1	2.9	797	26.4	0.7	835	50.2	1.0	808	20.0	3.4	809	16.4	2.9	808	$tCH_2+\gamma$OCO
32	834	41.5	4.6	801	30.4	4.8	803	19.1	8.5	844	41.8	2.7	814	31.8	0.5	810	36.5	2.5	820(836)	γC-H
33	925	5.6	2.3	897	52.7	0.9	911	48.9	0.4	925	3.7	1.9	899	56.7	0.9	912	48.3	0.5		ωCH_3+ ring νN-O
34	938	66.1	0.2	916	0.4	2.3	916	1.3	2.1	944	65.3	0.8	916	0.4	1.6	916	5.9	1.5	913	$\rho CH_2+\nu$C-CH_3
35	951	1.7	9.3	933	9.5	11.3	937	10.3	10.3	955	6.0	8.0	937	9.6	11.8	940	11.4	10.4	927	$\omega CH_3+\beta$C-H+βCNC
36	989	0.8	3.7	946	29.1	0.5	941	33.5	0.6	995	1.1	3.8	952	31.3	1.1	945	33.1	1.4	945(955)	ωCH_2
37	1011	9.7	6.9	969	0.2	0.7	975	1.2	0.8	1012	13.3	6.0	973	0.2	0.8	978	1.3	0.6	972	$\omega CH_3+\beta$C-H+ring νC=O+βONC
38	1017	41.3	3.0	989	6.4	6.3	982	7.2	5.1	1015	33.0	3.4	992	9.1	3.9	983	11.1	4.2		$\omega CH_3+\rho CH_2$
39	1017	23.1	10.3	991	23.5	11.9	989	33.3	14.1	1021	29.7	11.6	995	17.7	13.2	994	29.3	14.1	1021(1025)	$\omega CH_3+\beta$C-H+βCCC
40	1040	4.9	0.4	999	7.2	2.0	995	1.8	2.0	1045	4.7	0.3	1004	9.8	1.3	998	1.1	1.6		$\rho CH_2+\omega CH_3$
41	1054	4.5	0.4	1012	5.0	2.1	1019	4.7	0.3	1057	3.7	0.4	1010	7.4	1.8	1019	4.0	0.2		ρCH_2+ring βCCC+νO=N

42	1061	0.1	2.2	1027	3.9	0.3	1025	0.5	0.8	1063	0.0	2.3	1030	3.4	0.2	1026	1.1	1.8		ρCH_2 of CH_3
43	1066	6.0	6.6	1034	0.4	0.8	1031	1.6	1.8	1073	7.1	7.3	1037	0.2	0.7	1027	1.4	0.6	1040	ρCH_2 of CH_3
44	1089	9.7	6.7	1054	3.6	4.3	1066	3.8	3.6	1090	11.5	6.7	1050	3.8	4.6	1062	4.7	3.9	1063	νO-CH_2+βN-H+βC-H
45	1139	3.4	1.8	1110	11.2	0.6	1108	9.1	0.6	1139	4.5	1.6	1112	22.5	0.5	1109	13.2	0.5		βC-H+νC-CH_3
46	1174	374.1	2.4	1141	489.1	4.5	1147	404.1	4.6	1171	414.8	2.5	1133	572.1	4.2	1141	492.0	4.2	1162	βN-H +βC-H+βOCO+ρCH_2
47	1214	192.7	2.3	1164	84.2	3.2	1171	112.7	2.8	1213	202.7	1.9	1160	44.8	2.3	1166	70.0	2.1	1180	βN-H +βC-H+νC=N+νC-O
48	1292	2.1	8.0	1255	38.8	12.6	1253	24.7	10.4	1297	165.9	7.6	1255	70.0	5.4	1259	36.7	8.3	1211(1214)	βC-H+Ring νC=O+ρCH_3+βN-H
49	1297	145.9	7.5	1259	34.7	3.4	1267	44.2	4.3	1299	11.0	4.8	1263	38.1	6.8	1263	44.0	3.3		tCH_2
50	1322	383.1	3.2	1275	159.5	8.4	1282	194.3	8.1	1318	342.6	3.1	1270	104.6	5.7	1276	164.4	6.0	1270(1272)	ρCH_2+νC-C+βC-H of CH_2
51	1393	14.1	17.4	1346	4.3	8.2	1340	2.5	7.3	1391	14.0	14.8	1346	3.2	6.3	1338	2.5	5.5	1306	ωCH_2+βN-H+νC-N
52	1396	15.1	6.3	1366	6.4	14.1	1354	12.0	14.3	1394	15.1	3.6	1365	9.0	10.6	1350	13.7	11.0		δ CH_2+ CH_3 bending
53	1405	1.7	3.7	1368	5.9	15.6	1358	4.2	16.0	1406	3.1	2.6	1368	4.2	8.4	1354	3.4	8.8		CH_3 bending
54	1419	18.9	23.2	1390	14.1	25.7	1380	11.9	23.5	1418	17.3	20.2	1387	14.4	21.8	1375	11.6	19.4		δ CH_2+ CH_3 bending
55	1442	77.9	37.9	1412	124.0	23.3	1401	24.6	21.4	1443	88.7	32.0	1411	103.4	23.7	1399	25.8	20.3		δ CH_2+βN-H
56	1445	6.3	15.5	1413	32.9	19.5	1419	8.4	16.9	1447	7.8	10.0	1413	93.2	17.8	1414	9.7	10.8		δCH_2+βN-H
57	1450	6.9	17.2	1429	7.2	17.2	1419	131.5	27.4	1450	8.8	11.1	1426	8.9	11.2	1415	7.9	11.1		δCH_2+βC-H of CH_3
58	1453	16.5	12.4	1431	4.6	15.4	1420	10.0	16.9	1456	13.9	11.0	1428	7.0	9.6	1419	156.3	26.9		δ CH_2+βC-H of CH_3
59	1466	51.6	7.8	1433	47.0	68.3	1426	24.3	43.9	1466	57.7	5.4	1430	35.9	68.5	1422	19.7	39.4	(1437)	δ CH_2+βC-H of CH_3
60	1470	159.0	3.0	1447	31.5	9.5	1436	34.6	9.8	1470	175.4	2.7	1445	37.3	6.8	1431	38.3	7.1	1442	δ CH_2+βC-H of CH_3
61	1489	220.7	12.2	1456	162.6	9.1	1466	194.3	18.6	1491	181.2	13.9	1454	11.4	0.4	1463	189.6	23.1	1477(1472)	δ CH_2+βN-H+Ring νC=C
62	1575	75.9	25.0	1526	177.5	68.9	1534	179.2	77.9	1575	74.6	25.5	1526	63.6	0.2	1533	174.7	76.6	1560(1563)	βN-H+Ring νC=C+νC=N+CH_3 bending
63	1677	395.6	7.3	1606	239.2	15.4	1612	255.6	16.8	1676	422.5	8.7	1604	12.6	0.6	1610	270.0	14.3	1625	Ring νC=C+νC=N+βN-H+CH_3 bending
64	1686	19.9	70.7	1646	32.9	70.0	1650	30.0	70.8	1681	11.0	78.5	1640	35.3	77.5	1645	32.1	79.4	1637(1640)	νC=C+δ CH_2
65	1798	350.0	0.3	1735	234.3	2.0	1749	240.3	2.5	1795	380.1	0.3	1731	261.3	1.5	1744	268.8	2.1	1700	νC=O+βN-H+δ CH_2
66	1811	153.5	14.0	1748	86.9	25.0	1761	92.2	25.5	1809	164.4	14.2	1744	95.6	27.5	1756	101.5	28.2	1728(1725)	νC=O+βN-H
67	2885	23.2	116.4	2932	14.6	118.2	2933	13.8	122.6	2888	23.1	132.2	2935	15.3	138.6	2933	14.0	140.7	1734	$\nu_s CH_3$
68	2891	16.6	168.3	2935	14.8	221.4	2938	13.2	225.0	2893	16.8	190.7	2938	15.0	256.8	2937	13.2	255.2	2937(2938)	$\nu_s CH_3$
69	2926	26.8	89.0	2947	23.8	93.2	2946	24.3	94.9	2933	28.7	91.4	2954	25.6	101.8	2949	25.5	102.0	2952	$\nu_s CH_2$
70	2943	21.5	70.5	2990	11.6	63.9	3001	9.3	65.1	2940	23.0	68.3	2987	12.6	65.5	2994	10.1	63.6		$\nu_{as} CH_2$ of CH_3
71	2950	12.2	96.6	2992	8.2	109.1	3004	6.2	109.3	2948	13.5	94.0	2989	8.8	112.7	2998	6.8	108.5	2991(2996)	$\nu_{as} CH_2$ of CH_3
72	2958	26.8	68.1	3002	4.7	60.8	3006	3.5	60.3	2956	28.2	70.8	3007	3.6	61.0	3007	2.8	60.2		$\nu_{as} CH_2$
73	2977	5.4	52.4	3014	19.6	74.0	3024	17.4	75.6	2975	13.8	60.0	3011	22.0	82.8	3018	18.9	81.0		$\nu_{as} CH_2$ of CH_3+νCH of CH_3
74	2977	13.2	56.5	3031	6.6	59.7	3042	5.0	60.5	2980	5.9	46.8	3027	7.4	62.4	3036	5.6	60.9		$\nu_{as} CH_2$ of CH_3+νCH of CH_3
75	3006	10.9	96.5	3045	7.1	108.4	3045	6.8	107.1	3001	11.0	102.1	3042	8.1	120.3	3039	7.4	115.7	3042	$\nu_s CH_2$
76	3092	2.8	61.2	3138	2.5	63.9	3141	1.9	63.5	3086	2.8	63.0	3132	2.6	70.2	3132	1.8	67.1	3105(3109)	$\nu_{as} CH_2$
77	3157	8.7	30.2	3199	6.6	28.8	3199	7.5	28.8	3153	8.6	29.7	3195	6.8	29.8	3192	7.8	29.1	3186(3191)	νCH
78	3493	65.1	50.4	3470	39.6	82.3	3483	43.8	81.7	3500	63.2	52.6	3478	41.0	87.1	3485	44.2	85.2	3274	νNH

FT-Raman values are given in parenthesis. [Frequency (cm^{-1}), IR intensities (Km/mol), Raman scattering activities (Å amu^{-1})]. ν, stretching; ν_s, sym. stretching; ν_{as}, asym. stretching; β, in-plane bending; γ, out-of-plane bending; δ, scissoring; ω, wagging; t, twisting; ρ, rocking; τ, torsion; def., deformation.

[a] Scaling factor (s.f.): 0.9026.

[b] s.f.: 0.9608.

[c] s.f.: 0.9584.

[d] s.f.: 0.9085.

[e] s.f.: 0.9668.

[f] s.f.: 0.9631.

vibrational assignments as well as IR intensities and Raman activities are given in Table 4. The proposed vibrational assignments are given in the last column of Table 4. Modes are numbered from smallest to largest frequency.

The comparisons of theoretical and experimental IR spectra indicate that the intense vibrations in the experimental spectrum are also intensive in theoretical spectrum. The calculated vibrational wavenumbers using different methods were compared with the experimentally observed values. Comparison of the frequencies calculated at HF and DFT (B3LYP and B3PW91) with the experimental values (Table 4) reveal the overestimation of the calculated vibrational modes due to neglect of anharmonicity in real system. Inclusion of electron correlation in DFT to a certain extend makes the frequency values smaller in comparison with HF frequency data [13]. Some bands found in the predicted IR spectra were not observed in the experimental spectrum.

The heteroaromatic structure shows the presence of C–H stretching vibrations above 3000 cm^{-1} which is the characteristic region for ready identification of this structure [22]. In this region, the bands are not affected appreciably by the nature of the substituents. The vibration mod 77 calculated to aromatic C–H stretch in the region 3153–3199 cm^{-1} is in agreement with experimental assignment 3186 cm^{-1} FT-IR (3191 cm^{-1} FT-Raman). The C–H in-plane bending vibration assigned at 1108–1139 cm^{-1} (mod 45) even though found to be contaminated by C–CH_3 stretch. The calculated frequency at 801–844 cm^{-1} for the C–H out-of-plane (mod 32) bending falls in FT-IR/FT-Raman value of 820/836 cm^{-1}.

In this study, FT-IR spectrum reveals a band at 2952 cm^{-1} in IAOEMA was assigned to CH_2 symmetric stretch. The CH_2 scissoring modes have been calculated IR bands at about 1445 and 1454 cm^{-1}. Thus similar bands at 1442 and 1477 cm^{-1} in FT-IR and 1437 and 1472 cm^{-1} in FT-Raman have been observed to the CH_2 scissoring vibration. The CH_2 wagging mode at 1346 cm^{-1} deviates positively by 40 cm^{-1} from the reported value of 1306 cm^{-1}.

A major coincidence of theoretical values with that of experimental evaluations is found in the symmetric and asymmetric vibrations of the CH_3 moiety (vibrations 68 and 71). The CH_3 antisymmetrical and symmetrical stretching occurs about 2900 and 2800 cm^{-1}, respectively. The symmetric stretching of CH_3 observed in FT-IR at 2937 cm^{-1} was calculated (mod 68) about at 2890 cm^{-1} at HF level, while DFT estimates it around 2938 cm^{-1}. The asymmetric CH_3 stretch (mod 71) calculated at B3LYP/6-31G(d,p) after scaling down gives the value of 2992 cm^{-1} is nearer to the observed value of 2991 cm^{-1}. But HF gives very low estimate of this frequency in the 2948 cm^{-1} region. The frequency 71 corresponds to the asymmetric stretch of methylene hydrogens of the methyl group.

The aromatic C=C stretching appears at about 1650 and 1450 cm^{-1} of spectrum. The C=C aromatic stretch observed in the region 1477–1625 cm^{-1} FT-IR spectra (1472–1640 cm^{-1} FT-Raman) are in agreement with theoretical assignment 1454–1604 cm^{-1} with DFT. The aliphatic C=C stretching band in the monomeric unit was observed at 1637 cm^{-1} FT-IR spectra (1640 cm^{-1} FT-Raman). The calculated C–C–C out-of-plane and in-plane bending modes have been found to be consistent with the recorded spectral values. The stretching of C–CH_3 (mod 45) computed in the range 1108–1139 cm^{-1} at HF and DFT levels is found to be with aromatic C–H in-plane-bending. The bending of C–CH_3 computed at 306 and 403 cm^{-1} with DFT is in agreement with experimental assignment 290 cm^{-1} (FT-Raman) and 417 cm^{-1} (FT-IR) values.

The medium absorption peak at 1180 cm^{-1} FT-IR spectra is attributed to the C–O stretch of the ester group. The peak (mod 47) was calculated at 1160 cm^{-1} with DFT/B3LYP. The amide and ester carbonyl stretching are shown at 1700 cm^{-1} (νNH—C=O) and 1728 cm^{-1} in FT-IR (1725 cm^{-1} in FT-Raman) (νO—C=O), respectively. The calculated stretching bands are in agreement with experimental values.

Because of the mixing of several bands, the identification of C–N vibrations is a very difficult task. Silverstein [22] assigned C–N stretching absorption in the region 1382–1266 cm^{-1} for aromatic amines. Sundaraganesan [23] assigned C=N and C—N stretching at 1689 and 1302 cm^{-1} in FT-IR spectrum, respectively. In the present work, the bands observed at 1306 and 1625 cm^{-1} in FT-IR spectrum have been assigned to C—N and C=N stretching vibrations. The computed values of C—N and C=N stretching vibrations also fall in the region 1338–1391 and 1604–1677 cm^{-1}.

The N–H stretching vibrations occur in the region 3200–3500 cm^{-1}. The scaled N–H symmetric stretch calculated at 3470 cm^{-1} and experimental value observed at 3274 cm^{-1} FT-IR. The N–H in plane bending and N–H out of plane bending are assigned to the bands at 1560 cm^{-1} in FT-IR (1563 cm^{-1} FT-Raman) and 598 cm^{-1} in FT-IR which agrees well with Sundaraganesan [23]. The calculated value for the N–H out of plane bending vibration is at 584–595 cm^{-1}. HF/6311G(d,p) is an excellent agreement with experimental observation (598 cm^{-1}). However, calculated value for the N–H in plane bending vibration at 1533 cm^{-1} deviates negatively by ca. 30 cm^{-1} from experimental observation may be due to the fact that it may be coupled with C=C and C=N ring stretching vibration.

5. Conclusion

In the present work, we determined the crystal structure of IAOEMA with X-ray diffraction analysis. FT-IR and FT-Raman spectra were recorded and the detailed vibrational assignments were presented for IAOEMA, for the first time. The molecular geometry, vibrational frequencies, infrared intensities and Raman scattering activities of IAOEMA in the ground state have been calculated by using ab initio HF and DFT (B3LYP and B3PW91) methods with 6-31G(d,p), 6-31+G(d,p), 6-31++G(d,p), 6-311G(d,p), 6-311+G(d,p), and 6-311++G(d,p) basis sets. The vibra-

tional frequencies were calculated and scaled values (with 6-31G(d,p) and 6-311G(d,p) basis sets) have been compared with experimental FTIR and FT-Raman spectra. The observed and the calculated frequencies are found to be in good agreement. The optimized bond lengths and bond angles show the best agreement with the experimental results.

Acknowledgement

This work was supported by the Scientific Research fund of Afyonkarahisar Kocatepe University. Project number 051.FENED.07.

Appendix A. Supplementary Material

Crystallographic data (excluding structure factors) for the structure of IAOEMA in this paper have been deposited with the Cambridge Crystallographic Data centre as supplementary publication number 651851. Copies of the data can be obtained, free of charge, on application to CCDC, 12 Union Road, Cambridge CB2 1EZ, UK [fax: +44 1223 336033 or e–mail:deposit@ccdc.cam.ac.uk].

Appendix B. Supplementary Material

Tables with other basis sets which are 6-31+G(d,p), 6-31++G(d,p), 6-311+G(d,p), 6-311++G(d,p) are available from the authors, on request.

References

[1] G. Odian, Principles of Polymerization, third ed., Wiley-Interscience, New York, 1991, pp. 198–334.
[2] S. Parker, M. Braden, Biomaterials 10 (1989) 91.
[3] I. Erol, J. Polym. Sci. Part A: Polym. Chem. 42 (2004) 3157.
[4] C. Soykan, I. Erol, Eur. Polym. J. 39 (2003) 2261–2270.
[5] C. Soykan, K. Guven, R. Coskun, J. Polym. Sci. Part A: Polym. Chem. 3 (13) 2901.
[6] A.P. Scott, L. Random, J. Phys. Chem. 100 (1996) 16502.
[7] S.Y. Lee, B.H. Boo, Bull. Korean Chem. Soc. 17 (1996) 760; N.C. Handy, C.W. Murray, R.D. Amos, J. Phys. Chem. 97 (1993) 4392.
[8] N. Sundaraganesan, S. Ilakiamani, H. Saleem, P.M. Wojciechowski, D. Michalska, Spectrochim. Acta A 61 (2005) 2995.
[9] G. Rauhut, P. Pulay, J. Phys. Chem. 99 (1995) 3093.
[10] M.J. Frisch et al., Gaussian 03, Revision B.4, Gaussian Inc., Pittsburgh PA, 2003.
[11] Rigaku, CrystalClear, Version 1.3.6. Rigaku American Corporation 9009 New Trails Drive, The woodlands, TX 77381-5209, USA, 2005.
[12] G.H. Sheldrick, SHELXS-97 and SHELXL-97, University of Göttingen, Germany, 1997.
[13] N. Sundaraganesan, S. Ilakiamani, B. Anand, H. Saleem, B.D. Joshua, Spectrochim. Acta Part A 64 (2006) 586–594.
[14] NIST Chemistry Webbook, IR database, http://srdata.nist.gov/cccbdb/.
[15] A. Frisch, A.B. Nielsen, A.J. Holder, Gaussview Users Manual, Gaussian Inc., Pittsburg.
[16] M. Kurt, Ş. Yurdakul, J. Mol. Struct. 654 (2003) 1–9.
[17] F. Yakuphanoglu, Y. Atalay, I. Erol, Mol. Phys. 103 (2005) 3309–3314.
[18] Y. Atalay, F. Yakuphanoglu, M. Sekerci, Spectrochim. Acta A 65 (2006) 964–968.
[19] B.G. Johnson, P.M. Gill, J.A. Pople, J. Chem. Phys. 98 (1993) 5612.
[20] Ş. Yurdakul, M. Yurdakul, J. Mol. Struct. 834–836 (2007) 555–560.
[21] N. Sundaraganesan, S. Ayyappan, H. Umamaheswari, B.D. Joshua, Spectrochim. Acta A 66 (2007) 17–27.
[22] M. Silverstein, G. Clayton Basseler, C. Morill, Spectrometric Identification of Organic Compounds, Wiley, New York, 1981.
[23] N. Sundaraganesan, S. Ilakiamani, P. Subramani, B.D. Joshua, Spectrochim. Acta A 67 (2007) 628–635.